Journal of Hydrology 575 (2019) 557–568

Contents lists available at ScienceDirect

Journal of Hydrology

journal homepage: www.elsevier.com/locate/jhydrol

Research papers

Dynamic changes of groundwater storage and flows in a disturbed alpine peatland under variable climatic conditions

Zhiwei Li[a,b], Peng Gao[c,*], Hanyou Lu[a]

[a] State Key Laboratory of Water Resources and Hydropower Engineering Science, Wuhan University, Wuhan 430072, China
[b] School of Hydraulic Engineering, Changsha University of Science & Technology, Changsha 410114, China
[c] Department of Geography, Syracuse University, Syracuse, NY 13244, USA

ARTICLE INFO

This manuscript was handled by Huaming Guo, Editor-in-Chief

Keywords:
Groundwater flow
Groundwater storage change
Water budget
Disturbed peatland
Climate change
MODFLOW

ABSTRACT

Climate change and gullies (and ditches) on peatlands are well known factors altering peat hydrology. Yet, exactly how this alteration emerges from interaction of these factors with groundwater dynamics is still not fully understood. In this study, we tackled this issue by coupling field measurement with model simulation using Visual MODFLOW. Groundwater processes and the associated water budget during five months of the wet season, 2017 were examined in the Zoige peatland, located on the northeastern side of Qinghai-Tibet Plateau, China with elevations of 3400–3900 m. Simulations were performed for a peatland area of 3.89×10^4 m^2 and three sub-zones within it representing peatland with no gullies (NG), a deep gully cutting through the peat layer (CT), and a shallow gully whose bed is within the peat layer (NCT). Model input parameters were calibrated and validated using the field-measured data. Modeling outcomes led to water budget showing relative contributions of main hydrological pathways (MHPs) (i.e., precipitation (*P*), evapotranspiration (*ET*), gully, groundwater flow, and boundary) to changes of water storage in peats (ΔS). Although these MHPs varied differently during rain and inter-rain periods, ΔS values were mainly controlled by the oscillated trend of the difference between *P* and *ET*. Variations of MHPs caused by NCT and CT were secondary to those due to those of *P* and *ET* during the wet season referred to as the short-term climate change. Vertical groundwater (VGW) flows were strongly correlated with water table (WT) levels in both rain and inter-rain periods, but their directions had different patterns in the two periods. Horizontal groundwater (HGW) flows tended to move into the deep (CT) gully, while move from the shallow (NCT) gully to the neighbor peats during both periods. Since HGW flows were about ten times greater than VGW ones, their effect on ΔS was significant during the long dry season. This would lead to continuous loss of groundwater stored in peats, demonstrating the coupled effect of long-term climate change and gullies on ΔS. These findings underline the necessity of controlling gully development and avoiding ditch excavation in future Zoige peatland management practices.

1. Introduction

The unique physical properties of peats make peatlands rich of water, carbon, and nutrient (Shi et al., 2015). Therefore, peatland degradation due to natural processes, such as climate change and development of gullies, and anthropogenic influence, such as ditch excavation and grazing, negatively affects peatland ecosystems and ecological functions (Holden et al., 2004; Wilson et al., 2011), particularly, those more vulnerable, such as the Zoige basin in the Qinghai-Tibet Plateau, China (Zhang et al., 2014; Zhang et al., 2016). Although degradation of peatland essentially refers to transformation of organics to inorganic mineral soils (decomposition) caused by biogeochemical processes and microbial activities (Holden et al., 2007; Ramchunder et al., 2009), these processes and activities are closely related to changes of peatland hydrology. For a given peatland unit (a site, plot, or catchment), peatland hydrology includes surface runoff, subsurface flow that mainly consists of macropore and pipe flows, and groundwater flow (Labadz et al., 2010). These flow paths are controlled by precipitation and evapotranspiration. Interaction between these flow paths and control factors drives the change of groundwater storage in peatland, which finally affects physical properties of peats (e.g., porosity, moisture contents, specific yield, and hydraulic conductivity) (Price and Whitehead, 2001). Therefore, determining groundwater storage and its change in peatland is essential for revealing the complex mechanisms that cause peatland degradation.

Theoretically, groundwater storage change (ΔS) for a given time

* Corresponding author.
E-mail address: pegao@maxwell.syr.edu (P. Gao).

https://doi.org/10.1016/j.jhydrol.2019.05.032
Received 18 February 2019; Received in revised form 5 May 2019; Accepted 8 May 2019
Available online 10 May 2019

interval is a function of peat specific yield (S_y) and the associated water table (WT) change assuming peatland is an unconfined aquifer. However, many field studies and modeling analyses indicated that values of S_y vary spatially and temporally not only among different peatlands but also within itself. Particularly, they vary along peat vertical profiles with inconsistent patterns among different peatlands (Price, 1992; Price, 1996; Ronkanen and Klove, 2005; Sumner, 2007). Moreover, WT varies spatially and temporally (Holden et al., 2011; Luscombe et al., 2016). The spatial variation may be due to topography at the local scale, or caused by natural gullies and artificial ditches, leading to the lateral dropdown effect and unevenly distributed WT levels on both sides of ditches. The temporal variation could be either varying between day and night or seasonally (Evans and Warburton, 2007). Thus, determining S_y and WT variation involve various uncertainties. In addition to these uncertainties, a more fundamental challenge lies in the fact that changes of WT can also be caused by peat expansion and compaction, which could contribute up to 60% of ΔS values (Kellner and Halldin, 2002; Price and Schlotzhauer, 1999). These uncertainties and challenges undermine the reliability of direct calculating ΔS in peatlands that have relatively large areas.

An alternative approach to determining ΔS relies on constructing water balance of a peatland (Fraser et al., 2001b; Price, 1996; Van Seters and Price, 2001):

$$P = ET + R + \Delta S + \varepsilon \quad (1)$$

where P is the precipitation, ET is the evapotranspiration, R is the runoff, and ε is the residual term. This approach implicitly assumes that the groundwater (GW) exchange is small, such that it may be ignored and lumped into the residual term (Evans and Warburton, 2007). Nonetheless, even during rainfall events, vertical GW exchanges may be measurable (Fraser et al., 2001a). In the inter-rain periods, the impact of GW flows on ΔS may not be negligible. For instance, diffuse seepage of GW was observed in ditches cutting through the peat layer (Rossi et al., 2012), suggesting relatively strong movement of GW flows, which may possibly contribute to ΔS. However, the interaction between GW flows and ΔS under the influence of ditches is apparently intricate and still not well known. Since natural gullies and/or artificial ditches are widespread in peatlands all over the world (Fisher et al., 1996; Gatis et al., 2016; Joosten et al., 2008; Labadz et al., 2010; Li et al., 2018; Ronkanen and Klove, 2005; Sikstrom and Hokka, 2016; Whittington and Price, 2006), understanding hydrological processes controlling this complex interaction is valuable for better managing peatland ecosystem (Dahl et al., 2007), particularly, in remote alpine peatland where deploying an intensive sampling campaign is often challenging.

In this study, we examined this interaction in a small peatland catchment in the Zoige basin, China using Visual MODFLOW model calibrated and validated by field measured data. Based on simulated results spanning over 124 days from May 17 to September 17, 2017, we elaborated quantitative contribution of each hydrological and climatic factor to water balance of the peatland. Then, we demonstrated different responses of ΔS to the climate change, represented as the rain and inter-rain periods, and gullies. which was followed by examining responses of both vertical and horizontal GW flows to these two factors. The study was closed by revealing the impact of long-term climate change and deep gullies on ΔS and GW flows. Our findings provided first-hand knowledge of groundwater hydrology in this rare alpine peatland that has not been studied from the process-based perspective.

2. Materials and methods

2.1. Study area

Zoige basin is situated in the Yellow River source region on the northeastern side of Qinghai-Tibet Plateau, China (Fig. 1a and b), where it develops the world's largest alpine peatland at the elevations of 3400–3900 m. The annual average rainfall of Zoige basin is about 765 mm, most of which is mainly concentrated in the June-September period. Since 1950s, the air temperature has increased by about 0.2 °C per decade, and the annual rainfall has varied with no distinct trend (Yang et al., 2017; Li et al., 2015). Evapotranspiration is related to land use types and climate change, ranging between 450 and 550 mm per year with a slightly increasing trend annually (Zhao et al., 2014). The area of Zoige peatland is about 5098 km^2, accounting for 49% of the total peatland area in China, and the organic carbon storage in this region is roughly 0.477 Pg, accounting for 32% of that stored in the Qinghai-Tibet Plateau (Wang et al., 2014; Wang et al., 2015). In addition, Zoige peatland stores groundwater up to several billions of cubic meters. Unfortunately, affected by climate change and human activities, Zoige peatland has experienced degradation since the 1950s with an annual degradation rate of about 10%, jeopardizing local aquatic ecosystems and water resources utilization in the Upper Yellow River system (Bai et al., 2008; Huo et al., 2013; Li et al., 2010; Yang et al., 2017). As ombrotrophic mires, Zoige peats are annually replenished by precipitation, and their stored water is reduced by evapotranspiration and further drained out by natural gullies and artificial ditches (Li et al., 2018; Li et al., 2015). Thus, understanding dynamic changes of stored groundwater in Zoige peatland is crucial for developing best management practices to stop degradation.

Our study catchment is located in a small tributary of the upper Black River with the area of about 0.151 km^2 (Fig. 1c). Its west and east sides are surrounded by hillsides, and the south side is the high end of this catchment. The mainstream of the catchment flows into the north from the southwest direction, converged by a few tributaries with variable sizes. Since all of the channels are developed on upland of the upper Black River, they may be geomorphologically treated as gullies. The peat layer within the catchment varies between 0 and 2 m thick, underlain by a sandy silt layer with the median diameter varying between 0.039 mm and 0.651 mm. In this study, gullies are divided into two categories. In the first category, deep gullies cut through the peat layer making their beds lower than the bottom of the peat layer and hence possibly allowing more groundwater to seep out from the boundary between the top peat and bottom soil layers. In the second one, shallow gullies have the bed whose depth is less than the peat layer thickness, such that the entire gully is within the peat layer. Hereafter, these two types of gullies are referred to as the CT (Fig. 1d) and NCT (Fig. 1e) gullies, respectively. According to this definition, the mainstream and the longest tributary are the CT gullies with the total length of about 1014.4 m, the mean width of 1–3 m, and the deepest depth up to 1.5 m, while others are NCT gullies with the total length of 1458.6 m and very shallow depths (Fig. 1c).

2.2. Data acquisition

We measured topography, peat layer thickness, WT levels, specific yield, and hydraulic conductivity in 2016 and 2017 in the study catchment. Using a differential GPS (Trimble R2) that has vertical and horizontal accuracies of ± 0.85 and ± 0.50 m, respectively, we collected 831 elevation points across the catchment and converted them using a Kriging interpolation method into DEM data that had a mean plane resolution of 13 m (Fig. 1c). Peats in the study area were generally deep in and near the valley and shallow toward the east and west edges with relatively steep slopes. We measured peat depths at 119 locations and interpolated them throughout the entire study area to obtain spatially variable distribution of peat thickness. Both DEM and peat depths in the simulation zone were used as a prototype for defining the simulated peat volume and constructing the conceptual model. We also measured WT levels within the study catchment using self-made dipwells, each of which was 110 cm long and 0.02 m wide in diameter, and was pushed or hammed into the peat for at least 1 m deep. On May 17th, 20th, and 23th, July 17th, and September 18th, WT levels at 114, 103, 105, 77, and 81 locations distributed within the student catchment were manually measured, respectively (Fig. 2a). Furthermore, several

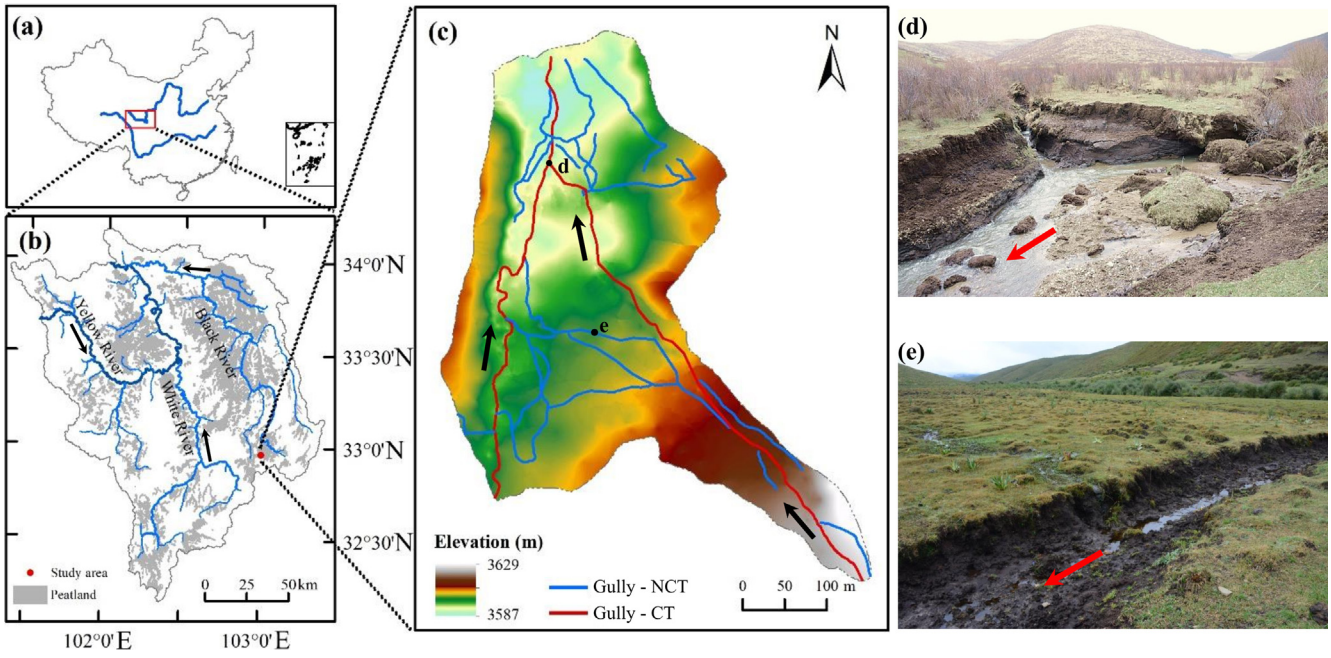

Fig. 1. Study area and two types of gullies in the Zoige basin. (a) and (b) Locations of the Zoige basin and the selected study area; (c) Topographic structure of the study area and gully network. NCT refers to the shallow gully whose bed is within the peat layer, while CT denotes the deep gully whose bed cutting through the peat later; (d) and (e) Illustration of a CT and NCT gully. The arrow represents flow direction. The locations of these two gullies were marked in (c).

automatic water loggers (HOBO) were installed in gullies and inserted under the peat surface to measured continuous WT levels (Fig. 2a). Some of these data were used to determine daily water levels in the gully and to create dynamic WT levels along the boundary of the simulation zone (i.e., the boundary conditions).

Specific yield (S_y) of peats was measured by taking a total of 36 samples from three different locations and in different peat depths using the method described by Price (1992). The measured S_y values did not show much variation along the peat depth and its mean among three locations ranged between 0.02 and 0.05. Hydraulic conductivity (K) was measured using self-made piezometers following the procedure laid out by Chason and Siegel (1986). This procedure does not distinguish horizontal from vertical K and thus is a comprehensive K. Measured values of K varied in the range of 0.35–0.89 $\times$ 10^{-6} m s^{-1}. Generally,

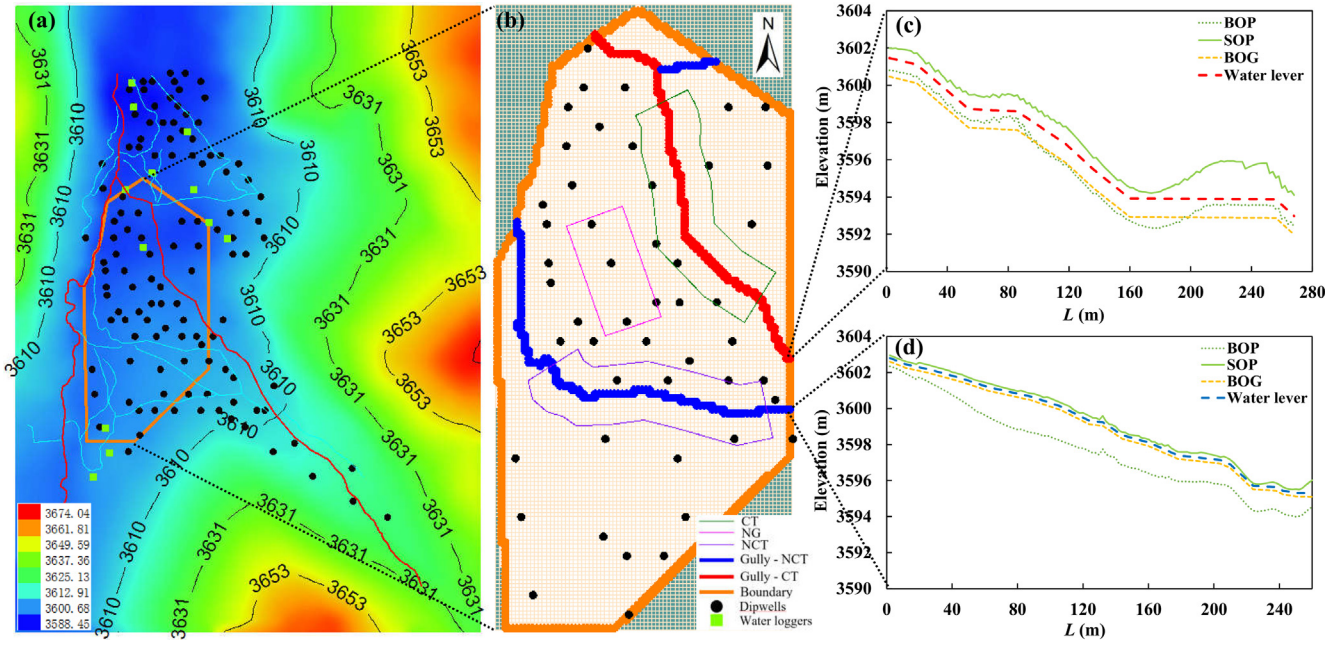

Fig. 2. The simulation area and conceptual model. (a) Location of the simulated area. The black dots (dipwells) are locations with field measured WT levels and the green dots (water loggers) are the locations where continuous WT levels were monitored; (b) Details of the conceptual model including two types of gullies, the boundary of the simulation zone, and three sub-zones, purple: NCT, pink: NG, and green: CT; (c) Longitudinal profiles of a CT gully. BOP: bottom of the peat layer, SOP: surface of the peat layer, BOG: bottom of the gully; and (d) Longitudinal profiles of an NCT gully. In the CT sub-zone, the gully cut through most portion of the peat layer, whereas in the NCT sub-zone, the gully is well within the peat layer. (For interpretation of the references to colour in this figure legend, the reader is referred to the web version of this article.)

the sandy silt layer beneath the peats has less permeability. Since the median size of the sandy silts was about 0.039 mm, the value of K should be between 1 and 2×10^{-5} m s^{-1} (Zheng and Bennett, 2002). Given that K in a silt layer is typically $10^{-1} - 100^{-1}$ times less than that in a peat layer (Ronkanen and Kløve, 2008), it is reasonable to set $K = 1 \times 10^{-8}$ m s^{-1} for the sandy silt layer.

2.3. Model overview

We used Visual MODFLOW (Modular Three-dimensional Finite-difference Ground-water Flow Model) to simulate groundwater movement within peatlands in the study catchment and construct water budget from May to September 2017 using modeling outcomes. This software has been widely used to simulate three-dimensional groundwater flow and pollutant transport due to its easy-to-use simulation environment (Bujakowski et al., 2014; Cruz-Fuentes et al., 2014; Grapes et al., 2006; Lautz and Siegel, 2006; Xue et al., 2018). It adopts a three-dimensional model equation of ground motion in porous media (Harbaugh et al., 2000):

$$\frac{\partial}{\partial x}\left(K_x \frac{\partial h}{\partial x}\right) + \frac{\partial}{\partial y}\left(K_y \frac{\partial h}{\partial y}\right) + \frac{\partial}{\partial z}\left(K_z \frac{\partial h}{\partial z}\right) - W = S_s \frac{\partial h}{\partial t} \quad (2)$$

where K_x, K_y, and K_z are the hydraulic conductivity (m s^{-1}) in horizontal, transverse, and vertical directions, h is the pressure head (m), W is the rate at which the source and sink flow input and output per unit time (s^{-1}), S_s is the unit water storage rate (m^{-1}), and t is the time (s). In the model, the simulated peatland is treated as a series of discretized three-dimensional cells and Eq. (2) is applied to these cells to simulate the temporal and spatial variations of continuous water volume within the peatland. The finite difference method was used in the model to obtain an approximate solution for each cell. If the solution may be achieved within a given error range, then an output stable water head is produced to represent average groundwater head around the cell. Simulation requires that each of these three-dimensional cells is set for soil parameters and initial water head distribution. Input parameters of the model include rainfall, evapotranspiration, boundary water head, topographic feature, geometrical information of gullies, hydraulic conductivity, specific storage, specific yield, effective porosity, total porosity, and initial water head. Results of model simulation lead to a water balance formula for calculating the net change of the groundwater in the peatland (i.e., groundwater storage change, ΔS):

$$\Delta S = P + ET + NBW + NGW - SR \quad (3)$$

where P is the total precipitation of the rainy season, ET is the total amount of evapotranspiration over the same period, NBW is the net change of the amount of groundwater in the boundary, NGW is the net change of the groundwater volume of peatland discharged by the gullies, and SR is the surface runoff in the rainy season.

2.4. Model setup and input data

Since the peat layer in the study catchment becomes thinner as moving toward locations with higher elevations on both western and eastern sides, modeling groundwater flow in these thin peats is very difficult, if not impossible. So, we selected a peat zone in the middle of the catchment as the modeling zone (i.e., prototype) with the area of 3.89×10^4 m^2 (Fig. 2a). Its boundary (Fig. 2b) was determined in terms of three reasons. First, it includes both types of gullies, which enables examining the impact of gullies on groundwater dynamics and groundwater storage changes. Second, it involves sufficient number of measured discrete water table (WT) levels, which may be used for model calibration and validation. Third, it contains several locations where continuous WT levels were recorded by HOBO Water Level Data Loggers, which allowed for the simulation under the transient head boundary condition. Peat thickness within the modeling zone varied between −2.90 m and 0.00 m, giving rise to the peat volume of 6.79×10^4 m^3. In the preliminary runs, the upper peat layer within the simulation zone was divided into a grid of cells whose size was 2×2 m and split vertically in two layers. This arrangement resulted in 160×76 cells with the density of 3.2/m^2, much less than that set by Brixel (2010) and Ronkanen and Kløve (2008), which was 80, and 9–25/m^2, respectively. Thus the spatial resolution of our model structure is relatively high. Unfortunately, modeling failed because simulation could not converge. As such, the whole peat layer was treated as one layer and discretized into a series of three-dimensional cubes with the size of 2 m^2 × d m, where d is the mean peat thickness within each cube. The underneath sandy silt layer was set with the thickness of 20 m. Therefore, the conceptual model is the peatland volume bounded by the orange polygon in Fig. 2b that contains the peat (upper) layer and soil (lower) layer.

Visual MODFLOW requires input of three parameters describing physical properties of peats in the simulation zone, S_y, K, and porosity (ϕ). Based on our field measurement, the value of S_y was set as 0.05 and specific storage (S_s) is 0.001 m^{-1}. Values of K we measured in the field were the comprehensive K. Thus, we assume $K_x = K_y = K_z = K$ and set it as 3.89×10^{-4} m s^{-1}. Values of effective and total porosity were not measured directly in the field. Alternatively, we set them as 30% and 80%, respectively, based on earlier studies (Heathwaite and Göttlich, 1993; Reeve et al., 2000). Peatland topography was represented by the mean elevation of each cube, which was determined by interpolating the field measured elevation points and taking the average for those falling within each cube. The initial boundary condition for simulation was represented by WT levels along the boundary, which were determined using the measured WT levels on May 17, 2017. Using time series of WT levels measured at several locations on the boundary, we created temporally variable WT levels along the boundary to provide the transitional head condition for model simulation. Elevations of the gully bed in the CT sub-zone were reconstructed based on field observation and measurements, showing that a large proportion of it (bottom of gully, BOG) was below the peat layer (bottom of peat, BOP) (Fig. 2c). In the NCT sub-zone, the BOG was well above the BOP (Fig. 2d). The initial water level in the CT gully was set as 1 m below the peat surface (SOP) and its variation during the simulation period was determined based on the water levels recorded by an installed water logger. In the NCT gully, it was set as 0.2 m below the SOP and varied between −0.03 and −0.23 m based on measured WT levels from a nearby dipwell during the simulation period.

Rainfall is the main water input in the Zoige peatland. In this study, hourly precipitation for the simulation period (i.e., may 17 – September 17, 2017) was approximated using the compiled precipitation data from the nearest weather station, Hongyuan County Meteorological Observatory (32.48° N, 102.33° E). Evapotranspiration (ET) in the simulation zone was also estimated from the same weather station using meteorological data, including temperature, sunshine hours, wind speed, air pressure, and relative humidity. Values of ET in wetlands have been widely calculated using a modified Penman-Monteith (P-M) formula, commonly referred to as the FAO56 P-M method (Abtew et al., 2011; Jacobs et al., 2002; Lott and Hunt, 2001; Mao et al., 2002; Wossenu, 1996). However, the ET value calculated in this way is only for a 'reference crop' defined as a hypothetical crop with a height of 0.12 m, a fixed surface resistance of 70 s m^{-1}, and a reflectivity of 0.23 (Allen et al., 1998). To calculate the true ET values for peatland, this one needs to be multiplied by a correction factor, C_p. Using independently determined C_p values, which vary seasonally (Li et al., 2013), we calculated hourly ET values for the simulating period (see detailed calculation in Li and Gao (2019), under review). Surface runoff is not specifically simulated in Visual MODFLOW. Instead, it is approximated by the Drain module imbedded in the model and estimated as a lumped amount of water moving out of the simulation zone without taking part in any hydrological process (Reeve and Gracz, 2008; Grapes et al., 2006; Reeve et al., 2000; Rossi et al., 2014). Therefore, this component was included in the subsequent water budget

calculation.

To understand gully impact on both ΔS and groundwater flows, we selected three sub-zones within the simulation zone (Fig. 2b). The CT sub-zone includes a proportion of the CT gully, the NCT sub-zone contains a proportion of the NCT gully, and the NG sub-zone has no gully within it at all. Their areas were 3605.99, 3594.46, and 1800.00 m^2, respectively. In addition to the entire simulation zone, Visual MODFLOW was also used in these three sub-zones for the same time periods with the same input parameters.

2.5. Model calibration and validation

The initial WT levels in the simulated area were set at the peat surface to allow free movement of groundwater from January 1 to April 24, 2017. Then, the available *P* and *ET* data were used as true input data and WT levels along boundaries were remained unchanged until May 17, the beginning of the formal simulation. This pre-modeling treatment provided sufficient time for groundwater to distribute within the sandy silt (i.e., lower) layer. The difference between calculated WT levels (*Cal*) and observed ones (*Obs*) was used to test the goodness-of-fit. Parameters required as input data in the model were calibrated by comparing the 48 and 31 pairs of *Cal* and *Obs* in the simulation area on May 17 and July 17, 2017, respectively (Fig. 3a). The resultant RMSEs were 0.27 and 0.20 m for the two days, respectively. Given that variation of WT levels could be more than 1 m (based on our measured continuous water table level data), these RMSE values are very low. In addition, the shape of the residuals suggests that there was no spatial autocorrelation that may affect the assessment (Burt and Barber, 2009). These calibrated parameters were subsequently validated using the measured WT levels in May 20 (34 points), May 23 (36 points), and September 17 (26 points), The RMSEs were 0.33, 0.31, and 0.12 m for the three days, respectively. Both these relatively low RMSEs and their error shapes (Fig. 3b) indicated that the model was robust for predicting WT levels and groundwater flows in the study area.

2.6. Analysis

Water budget that included net input and output of hydrological components was analyzed for both the entire simulation zone and three sub-zones. The short-term climate change during the simulation period (i.e., the wet season) was reflected by net water change from the air, which was quantitatively expressed as the difference between *P* and *ET* ($W_{P\text{-}ET}$), To specifically characterize its impact on both ΔS and groundwater flow, the entire simulation period that amounted to 124 days was divided into a group of rain periods and that of inter-rain periods based on temporal distribution of precipitation. In addition, all these small periods were further categorized into four classes based on the nature of the distributed *ET* values, class 1: $ET \leq 2$ mm, class 2: 2 mm $< ET \leq 3$ mm: class 3: 3 mm $< ET \leq 4$ mm, class 4: $ET > 4$ mm. Water budget was subsequently analyzed during these two distinct periods to show different responses of ΔS to rain and inter-rain periods. Groundwater flows were examined in the vertical direction between the peat layer and its underlying sandy silt layer, and the horizontal direction in the peat layer. Vertical groundwater (VGW) flows in the four *ET* classes were compared among each other and linked statistically to the associated WT levels during the two types (i.e., rain and inter-rain) of periods for not only the entire simulation peat zone, but also three small sub-zones. Horizontal groundwater (HGW) flows were examined only for the CT and NCT sub-zones to reveal their responses to the two different types of gullies along the lateral distances away from the two gullies.

3. Results and analysis

3.1. Water storage change and its dynamic variations

3.1.1. The entire simulation zone

During the study period (5/17/2017 – 9/17/2017), the dominant water input was precipitation (*P*), taking 97.42% of the total input. This left only 2.58% supplied from the boundary as groundwater (GW) flow (Fig. 4a). The amount of lost water from the peats was largely from evapotranspiration (*ET*) (71.62%). About 21.03% of it was in the form of surface runoff, flowing out of the simulated peatland area. Gullies developed within the simulated peatland area drained as GW flow about 7.35% of the total out of the system. These hydrological paths resulted in the increase of water storage by 487.64 m^3, taking about 2.73% of the original stored water (i.e., that on May 17, 2017) in the simulated peatland body. These values showed that *P* and *ET* were clearly two dominant factors controlling the change of groundwater storage (ΔS). During the inter-rain periods, input water to the peat layer was predominantly from groundwater moving in from outside of the simulation zone through the boundary and the gullies, taking 58.43% and 38.39%, respectively (Fig. 4b). Water loss was almost all due to *ET*. The net result was the reduction of stored water (i.e., ΔS) by 2359.47 m^3, taking about 13.20% of the original ΔS value.

For all individual rain periods, the mean ΔS values were not correlated with the four *ET* classes (Fig. 5). Although they were statistically similar based on the analysis of variance (ANOVA) test, individual ΔS values, in particular, those in the highest *ET* class, may vary greatly. For the inter-rain periods, all ΔS values and their means in the four *ET* classes were less than zero (Fig. 5) and their means remained statistically similar. Clearly, ΔS values were more variable in the rain periods than in their counterparts (Fig. 5).

3.1.2. The three sub-zones

Although *P* was still the dominant water input source during the

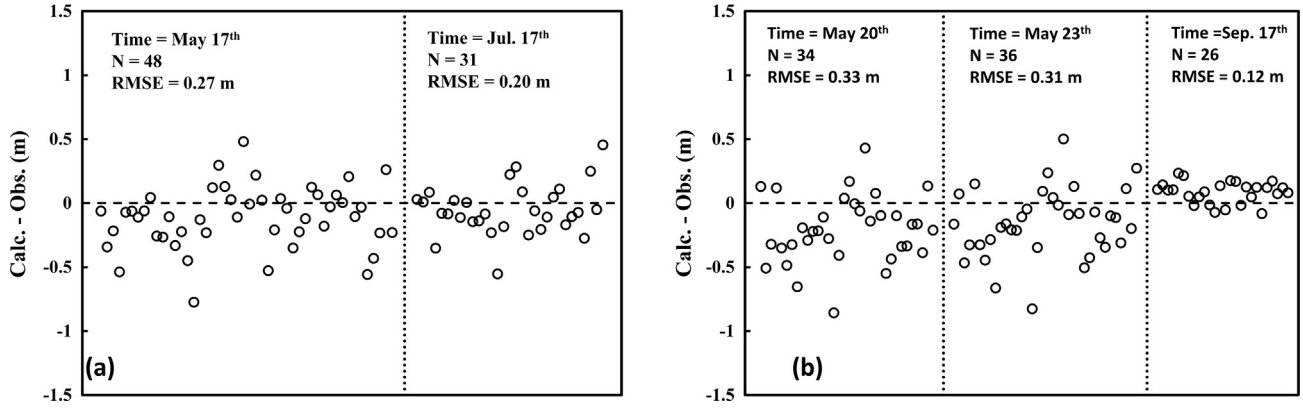

Fig. 3. Model calibration and validation. (a) calibration results using the measured data on May 17 and July 17, 2017; (b) validation results using the measured data on May 20, 23, and September 17, 2017.

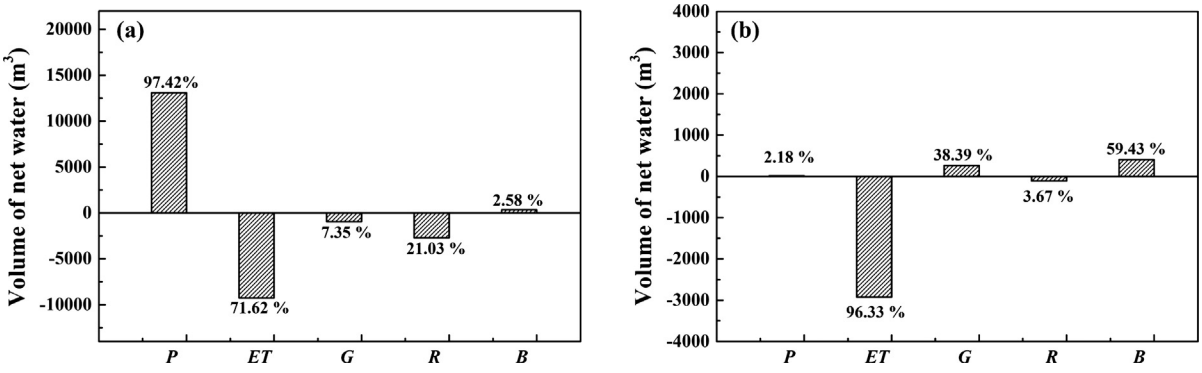

Fig. 4. Water budget analysis based on model results for the entire simulation zone during (a) the whole simulation period and (b) the inter-rain periods. P: precipitation, ET: evapotranspiration, G: gully, R: surface runoff, and B: boundary. Positive components are water input, while negative ones are water output, and the difference of the water volume is the change of water storage in peats.

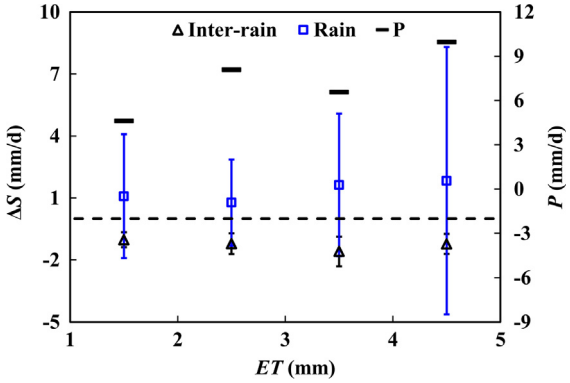

Fig. 5. Simulated means and variations of daily Δ*S* and precipitation (*P*) for the rain and inter-rain periods in the four *ET* classes.

whole periods, its contribution to the three sub-zones varied from 100% in the NG to 86.36 and 86.55% in the CT and NCT sub-zones, respectively (Fig. 6a). The latter were obviously different from that of the entire simulation zone. The remaining 13.84% to the CT sub-zone was supplied from the boundary, while that of 10.45% in the NCT sub-zone was supplied from the gully. The main water loss was also primarily contributed from *ET* with 72.54% and 72.03% in the NG and NCT sub-zones, respectively. This pattern was similar to that of the entire zone, but only 48.05% of the total loss was from *ET* in the CT sub-zone (Fig. 6a). The second largest water loss was from surface runoff in the NG, from the gully in the CT, and from the boundary in the NCT sub-zones, taking about 20.03%, 42.32%, and 18.50%, respectively. Because WT levels in the CT gully were measured *in situ*, these values measured during rainfall periods were indeed mostly contributed from surface runoff because overland flow moves much faster than GW flow. Yet, the NG sub-zone lost water from the boundary by 7.43%, while the CT sub-zone received water via the boundary. Thus, different types of gullies apparently alter distributions of hydrological components in peatland differently. These differences collectively led to different values of Δ*S* in the NG, CT, and NCT sub-zones, which were 6.35%, 3.17%, and 3.95%, respectively, signifying that gullies in peatlands could also change the variations of water storage in peats.

The impact of gullies on hydrological components in peats also prevailed in the inter-rain periods. The NG sub-zone had no input water at all, while small amount of water moved into the CT sub-zone from boundary (65.62%) and the gully (32.86%), and much more water was seeped through the gully into the NCT sub-zone (Fig. 6b). Although *ET* was the main pathway of water loss for all three sub-zones, 10.26% and 23.25% of the total loss was still through the boundary in the NG and NCT sub-zones. Consequently, the inter-rain periods caused the decrease of Δ*S* by 78.56, 32.67, and 47.04 mm in the NG, CT, and NCT sub-zones, taking 16.37%, 6.81%, and 9.80% of the original Δ*S* value, respectively. It should be noted that gullies played different roles during the rain and inter-rain periods. The NCT gully supplied water to the sub-zone in both periods with a higher contribution during the inter-rain periods (Fig. 6a and b). The CT gully received water from the sub-zone during the rain periods, while supplied water to the sub-zone during the inter-rain periods. Among the three sub-zones, Δ*S* values were not well correlated with the four *ET* classes (Fig. S1), which is similar to the case for the entire study watershed, suggesting that *ET* and gullies had independent impact on hydrological components and Δ*S* in peats.

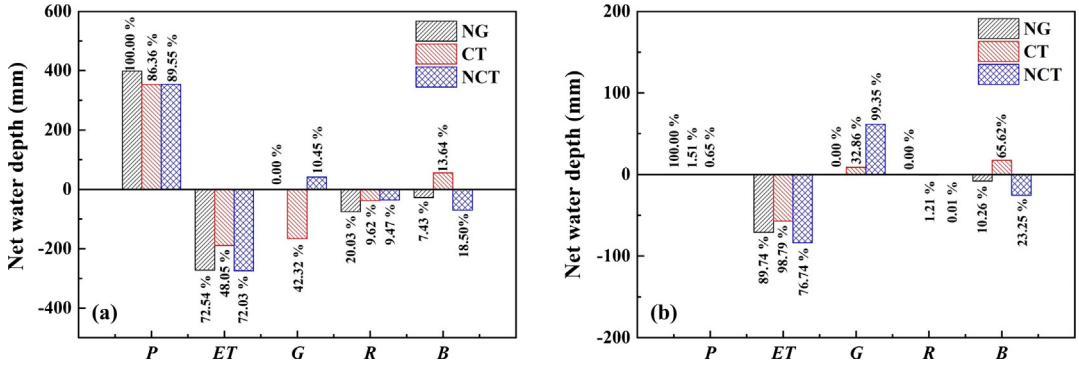

Fig. 6. Water budget analysis based on model results for the three sub-zones during (a) the whole simulation period and (b) the inter-rain periods. Net water depth was calculated as the ratio of net water volume to the associated sub-zone area, which allowed it to be comparable among the three sub-zones.

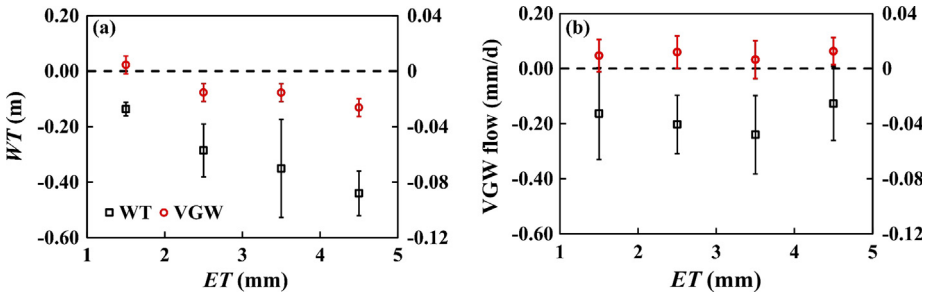

Fig. 7. Mean and variation of water table (WT) levels in the four ET classes during (a) inter-rain periods, and (b) rain periods.

3.2. Changes of water table levels and groundwater flows

3.2.1. Vertical groundwater (VGW) flows over the entire simulation zone and three sub-zones

Over the entire simulation zone, the mean water table (WT) levels during the inter-rain periods decreased quickly from 0.14 to 0.45 m below the peat surface with the increase of the *ET* classes, showing a clear correlation between the two variables (Fig. 7a). During the rain periods, however, the mean WT levels did not change with the *ET* classes and remained in a range between 0.13 and 0.24 m below the peat surface (Fig. 7b). ANOVA test showed that they were statistically similar. Their pattern over the four *ET* classes was indeed very similar to that of the mean precipitations in the same classes.

During the inter-rain periods, the mean VGW flows in the four *ET* classes showed a similar trend to that of the mean WT levels (Fig. 7a). In the lowest *ET* class, the VGW moved downward with a very small rate, but it reversed the flow direction in the remaining higher *ET* classes and gradually increased with the increase of *ET*. During the rain periods, all of the mean VGW flows in the four *ET* classes moved downward (Fig. 7b), which was very different from those during the inter-rain periods. Yet, these values showed a similar pattern to those of WT levels in the four *ET* classes, indicating a general correlation between *WT* values and VGW flows, the positive relationship only appeared during the inter-rain periods. These correlations may be further confirmed by strong linear relationships between VGW and ET for both inter-rain and rain periods (Fig. S2). Nonetheless, the magnitudes of these mean VGW flows were very low, ranging between 0.009 and 0.013 mm d^{-1}. Comparing with them, the means of VGW flows in the inter-rain period were mostly greater, ranging between 0.015 and 0.026 mm d^{-1}, except that in the first *ET* class, which was 0.004 mm d^{-1}. Therefore, the VGW flows at the larger spatial scale were generally small, but they were well correlated with WT levels.

During the inter-rain periods, the mean WT levels were negative in all three sub-zones with the lowest ones emerging in the CT sub-zone (Fig. 8a). In addition, they decreased at a similar rate in the NCT and NG sub-zones, while remained almost unchanged in the CT sub-zone (ANOVA test was not significant) (Fig. 8a). The discernable different patterns of WT levels between the former (i.e., the NCT and NG sub-zones) and the latter also echoed in their VGW flows. For the NCT and NG sub-zones, the means of VGW flows had very similar patterns (Fig. 8b). In the lowest *ET* class, they moved downward with relatively low rates, while in other higher *ET* classes, they changed the direction moving upward, Yet, the means of the VGW flows for the CT sub-zone in the four *ET* classes remained roughly unchanged (Fig. 8b). The similar patterns between mean *WT* values and means of VGW flows indicated their correlations that may be evidenced by their linear relationships in all three sub-zones (Fig. S3), consistent with that for the entire study area (Fig. S2),

During the rain periods, the WT levels and mean VGW flows demonstrated different trends (Fig. 8c and d). The WT levels were still the lowest in the CT sub-zone, while higher, but showing no trend with the four *ET* classes in the NCT and NG sub-zones (Fig. 8c). Although VGW flows for the CT sub-zone were still obviously different from those in the other two sub-zones, they slightly increased with the increase of the *ET* classes (Fig. 8d). Furthermore, VGW flows for the NCT and NG sub-zones moved downward for all *ET* classes with relatively high rates. Both changes of VGW flows and WT levels tended to be driven by the changes of mean *P* values in the four *ET* classes. Overall, these results showed the distinct impact of deeper (CT) gullies on both WT levels and VGW flows.

3.2.2. Horizontal groundwater flows around the CT and NCT gullies

Horizontal groundwater (HGW) flows showed variable trends between the two types of gullies in the four *ET* classes during the inter-rain periods (Fig. 9). In the lowest *ET* class, the HGW flows at the distance very close to the CT gully, moved into the gully with the highest rates. As the distance away from the gully on both sides increased, the HGW flow continuously moved toward the gully, but with decreased rates (Fig. 9a). Along the lateral direction of the NCT gully, the HGW flow still moved into the gully within the distance about 8 m away from the gully, but the rates of the flow were much less than those around the CT gully (Fig. 9a). As this distance further increased, the HGW gradually switched its flow direction, moving away from the gully. This lateral trend was obviously different from that around the CT gully.

In the second and third *ET* classes, the HGW flow generally moved toward the CT gully along the lateral distance away from it (Fig. 9b and c). Also, the HGW flows changed little with their means similar in the two *ET* classes. Around the NCT gully, the HGW flow commonly moved away from it with the flow rate higher at the location closest to the gully and lower in other locations. In the highest *ET* class, the HGW at the location closest to the CT gully flowed away from it with a relatively small rate (Fig. 9d). As the distance away from the CT gully increased, the HGW flow gradually reduced to zero and then slightly moved toward the gully. The HGW flow around the NCT gully, however, moved away from the gully in all modeled locations within 15 m away from the gully (Fig. 9d). The flow rate was relatively high at the location closest to the gully and then reduced moving away from the gully. There was no clear trend between the spatial patterns of the HGW flows and the *ET* classes.

During the rain periods, the mean HGW flows along the lateral distance away from the CT gully were generally higher than those around the NCT gully (Fig. 9e–h). In the four *ET* classes, the mean HGW flows demonstrated a similar pattern: starting with a high value at the closest location, decreasing quickly till the location of 9 m away from the CT gully, and gradually decreasing further with a lower rate. The HGW always flowed toward the CT gully, even in the highest *ET* class. Around the NCT gully, the decreasing pattern of the mean HGW flows was also similar among the four different *ET* classes with the HGW changed the flow direction at the location roughly 9 m away from the NCT gully. In all four *ET* classes, the variation around the mean HGW flows was the highest at the closest location to the CT gully (Fig. 9e–h) and then decreased quickly moving away from the gully. Around the NCT gully, the variation of the HGW flows at the closest location was

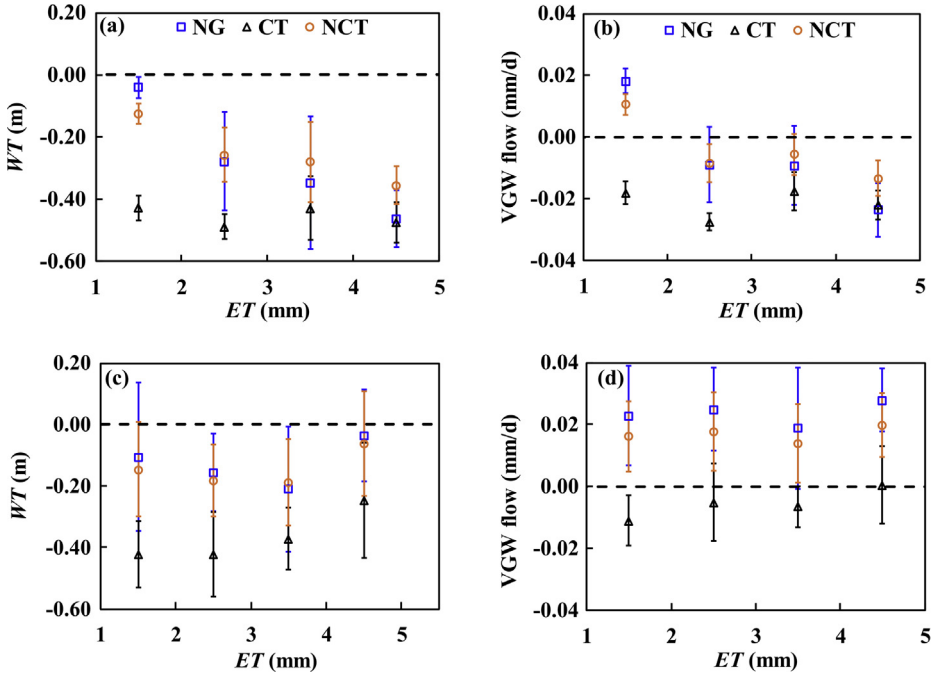

Fig. 8. Mean and variation of vertical groundwater (VGW) flows water table (WT) levels in the four ET classes during the inter-rain periods: (a) and (b), and the rain periods: (c) and (d).

still the highest one among that along the lateral distance, but was less than that around the CT gully at the same location. In general, the HGW flow moved toward the CT gully and its magnitude either decreased or remained unchanged as the distance away from the CT gully increased.

4. Discussions

4.1. Model limitations and sensitivity analysis

As a crucial parameter in groundwater modeling, hydraulic conductivity, *K* varies greatly in peats (Cunliffe et al., 2013; Holden and Burt, 2003). Unfortunately, it is very hard to directly measure its spatial distribution. Our attempts of using the subroutine in Visual MODFLOW (i.e., PEST) to create anisotropic and heterogeneous *K* values within the peat layer were not successful because simulations could not converge. Alternatively, we treated *K* values isotropic as many previous studies did and homogeneous as did in others (Molina et al., 2013; Reeve and Gracz, 2008; Ritzema and Jansen, 2008; Ronkanen and Kløve, 2008). Given that our measured *K* values at different peat depths and different time were variable (Table 1), we chose to determine the appropriate *K* value for the model from the result of sensitivity analysis in which measured WT levels were compared with predicted ones for each of the *K* values within the measured range (Fig. 10). On May 17, 2017 and July 17, 2017, the difference between predicted and measured WT levels increased generally with *K*, but within a limited range. Increase of the *K* value by more than three times (i.e., from 2 to 7 $\times$ 10^{-6} m s^{-1}) would lead to no more than 42% increase of the difference. On September 17, 2107, the same increase of *K* values led to the decrease of the difference, but only by 14%. These trends indicated that (1) errors in prediction (i.e. the differences) were not very sensitive to the change

Table 1
Measured saturation hydraulic conductivity at three depths, K.

Depth	K (cm/s)			Mean
cm	1	2	3	
40	0.00378	0.003725	0.002954	149E−03
72	0.000261	0.000301	0.000612	3.91E−04
100	0.000952	0.000086	0.000129	3.89E−04

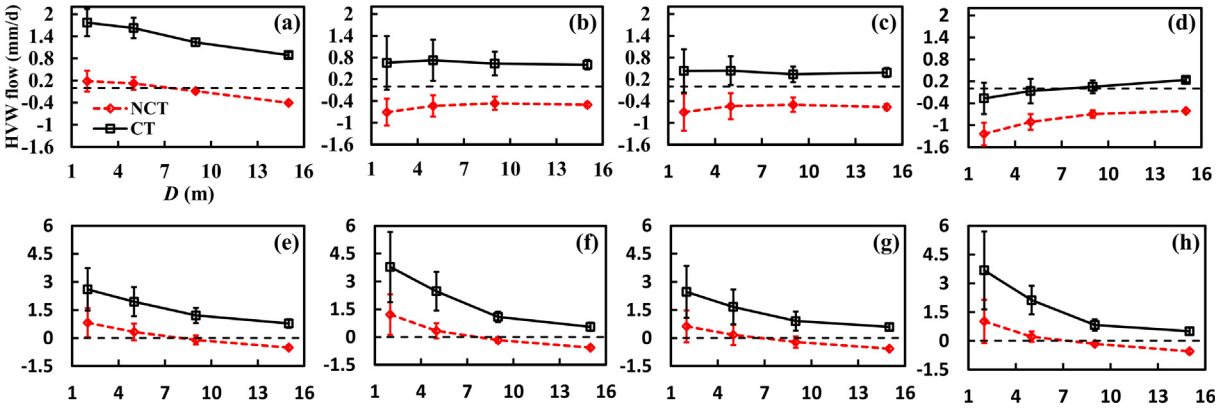

Fig. 9. Trends of horizontal groundwater (HGW) flows along the lateral distances away from the CT and NCT gullies for the four ET classes during the inter-rain periods ((a), (b), (c), and (d)) and the rain periods ((e), (f), (g), and (h)).

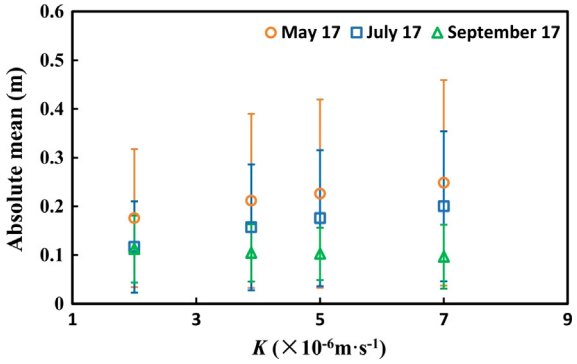

Fig. 10. Sensitivity analysis for hydraulic conductivity (*K*).

of *K* values, which was consistent with an earlier study (Ritzema and Jansen, 2008); and (2) the trends of errors were not always consistent over time. Thus, $K = 3.89 \times 10^{-6}$ m s^{-1} should be the most appropriate one.

Although determining surface runoff using the Drain module imbedded in Visual MODFLOW has been a common method (Grapes et al., 2006; Reeve and Gracz, 2008; Reeve et al., 2000; Rossi et al., 2014), it implicitly ignored a proportion of runoff moving into gullies within the study watershed during rainfall periods. However, water levels of flow in gullies used in the model were measured *in situ*, which had included this proportion of runoff. This inconsistency could lead to some errors in computation of water balance. Fortunately, the temporal changes of water levels during the entire simulation period were within ± 0.2 m, which mainly happened during rainfall periods. Thus, this uncertainty would cause limited errors in determining Δ*S* values.

4.2. Climatic and gully impact on water storage in the disturbed peatlands

For the entire simulation zone, the amount of supplied groundwater from ambient areas only took about 3% of the total input water during the rain periods, but more than 59% during the inter-rain periods (Fig. 4a and b). Nonetheless, in both periods, either *P*, *ET* or both dominated hydrological input and output. Thus, values of Δ*S* were mainly controlled by relative magnitudes of *P* and *ET* (i.e., the difference between *P* and *ET*, $W_{P\text{-}ET}$). Vicissitudes of rain and inter-rain periods in the wet season (May-September), which represents short-term climate change, could cause oscillation of Δ*S* between positive and negative values (Fig. 11). During the rain periods, the greater the $W_{P\text{-}ET}$ value, the greater the increase of water storage, while during the inter-rain (i.e. dry) periods, *ET* caused the loss of water storage, but the magnitude of the loss was not only controlled by *ET* values. For instance, groundwater input could be an important contributing factor as

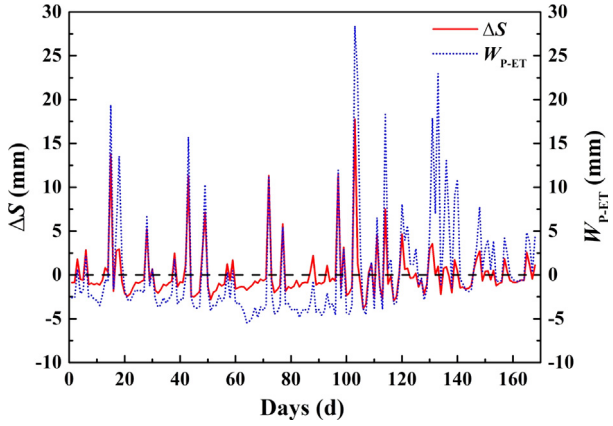

Fig. 11. Daily values of Δ*S* and $W_{P\text{-}ET}$ during the whole simulation period.

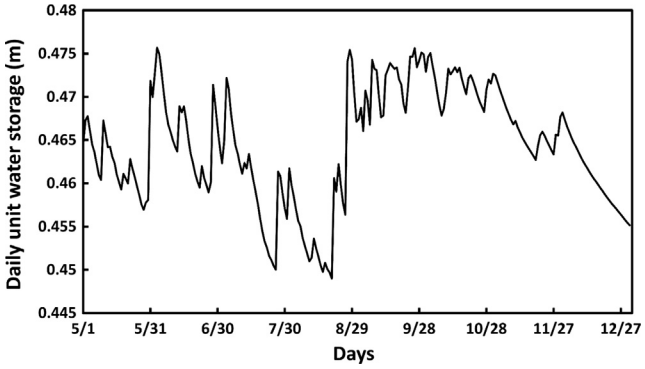

Fig. 12. Daily unit water storage (m) calculated as the volume of daily water storage divided by the simulation area.

shown in Fig. 4b. The opposite trends of Δ*S* between rain and dry periods gave rise to a very complex temporal pattern of Δ*S* – that is, it altered temporally between positive and negative over the whole modeling period (i.e., 124 days).

To understand these temporal changes over a long time period, we calculated the actual daily amount of water stored in peats as follow. After interpolating the measured WT levels on May 17, 2017 using a Kriging method, we obtained the initial spatially distributed WT levels in the study watershed and subsequently calculated the volume of the saturated peats, which was 596000 m^3. Assuming the effective porosity is 30% (Heathwaite and Johnes, 1996; Reeve et al., 2000), and pore water in the unsaturated upper peat layer is negligible, we could determine the initial amount of stored water (S_0), which was then unified by dividing the area of the study watershed (i.e., 38859 m^2). Using S_0 and Δ*S*, temporal changes of water storage may be finally determined up to the end of December 2017 (Fig. 12), which clearly signified that the amount of water stored in the peat layer highly varied from time to time, though the degree of variation was no more than 5.6%. Given that the annual climate change of the study area (i.e., the Zoige basin) is featured by the cycle of dry and wet seasons, this result (i.e., Fig. 12) may be repeated for many years and thus provided a reasonable projection on the impact of long-term climate change on water storage in peats. Nevertheless, whether this degree of variation may have significant ecological impact on the peat degradation is yet unclear (Putra et al., 2018).

During the full modeling period, water storage increased in all three sub-zones, suggesting that the impact of climatic changes (i.e. $W_{P\text{-}ET}$) on water storage in peats is greater than that of gullies. Furthermore, during the dry periods with *ET* values in the three high classes, the decreasing rate of storage water in the NG sub-zone was higher than that in the NCT sub-zone, which was higher than that in the CT sub-zone (Fig. S1). This apparently suggests that the disturbed peatland lost less stored water than the blanket peatland under the similar dry weather conditions, which is at odds with our field observation that in many CT gullies, groundwater seepage is discernable from the gully banks around the bottom of the peat layer (Li and Gao, 2019), indicating greater loss of stored water in peats. We can examine this phenomenon from a different perspective. Over the dry periods, both CT and NCT gullies supplied water to their surrounding peats and the NCT gully supplied much more water than the CT gully (Fig. 6b), suggesting that flow depths in the gully on average were higher than hydraulic heads of the neighboring peats and this difference was greater in the NCT than in the CT gully. The fact that gullies (both CT and NCT) in the entire simulation zone supplied a significant amount water to the surrounding peats (Fig. 4b) suggested that the hydraulic gradient from gullies to the neighboring peats prevailed over the entire simulation zone during the dry periods. The possible explanation is that sufficient water was supplied to the gullies during the rain periods, such that gully flows were capable of retaining at relatively high levels during the

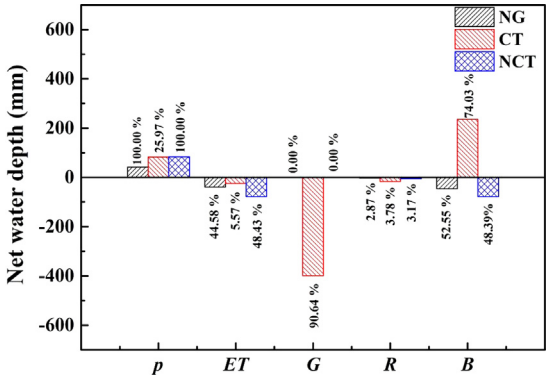

Fig. 13. Water budget analysis for the entire simulation area during the extended period.

dry periods, despite of precedent fast draining. This kind of hysteresis effect may be further corroborated by the fact that HGW flowed from the gully to the simulated peats most of time (Fig. 9).

However, this trend of hydraulic gradient gradually diminished as the dry periods continued. Our calculation of water balance for the 11/1-12/31/2017 showed that both *P* and *ET* were small due to dry and cold weather and thus had much less influence on water balance of the peatland. Under this condition, the CT gully was the main pathway of water output from the peatland even if water was supplied to it from its ambient areas, while the NCT gully did not have significant net water movement (Fig. 13). Thus, a higher amount of stored water decreased in the CT sub-zone (35.67 mm) than that in the NCT (29.35 mm) and NG (21.76 mm) sub-zones. This extended analysis reveals the impact of long-term climate change on peat groundwater storage, specified as follow. First, the role of CT gullies in draining additional stored water in peats takes effect over the prolonged dry period in winter and spring in the Zoige basin. Second, NCT gullies have very limited effect on ΔS. Thus, it is very important to control development of deep gullies for restoring peatland ecosystem.

4.3. Climatic and gully impact on groundwater flow in the disturbed peatland

Our results showed that HGW was about 10 times higher than VGW. This suggests that groundwater exchange between the peat (i.e., upper) and soil (lower) layers is not the main hydrological process affecting water storage in peats, possibly due to the fact that the study peatland is topographically controlled by a relatively steep slope (Hare et al., 2017; Millar et al., 2018). Yet, both VGW and HGW were subject to the coupled impact of climate change and gullies. Over the entire simulation zone, VGW flows were downward during the rain periods with very low rates and mostly upward with the rate increasing as *ET* increases. These patterns were essentially controlled by WT levels that demonstrated similar patterns, suggesting that the impact of climate change on VGW flows was achieved by altering WT levels, which essentially changed vertical hydraulic heads of peats (Li and Gao, 2019).

Although the strong WT-VGW correlation in the three sub-zones suggests that the controlling role of WT on VGW was not changed by gullies (either CT or NCT), the impact of gullies on the VGW flows was evidenced by the consistent patterns of VGW flows among the three sub-zone in both rain and dry periods: VGW flows in the CT sub-zone always moved upward even during the rainfall periods when these flows moved downward in NCT and NG sub-zones. This means that the hydrological role of the CT gully is lowering WT levels by allowing more groundwater seep into it, such that hydraulic heads in the peat layer was mostly lower than that in the underlined soil layer. The climatic impact adding to that of gullies on VGW flows was highlighted by much higher upward VGW flows in the dry periods than in the rainfall periods for the CT sub-zone, and inversion of VGW flow direction between the upward and downward directions during the two types of periods for NG and NCT periods.

Inasmuch as groundwater flow is dominated by HGW flows, their variations under the influence of both climate change and gullies should be more important for understanding dynamic changes of water storage in peats. Gullies clearly affected HGW flows along the lateral distance away from them. In general, HGW flowed toward the CT gully during both rain and dry periods, but it decreased as the distance away from the gully increased with the rate of decrease declined obviously after the distance about 8 m away from the CT gully (Fig. 9). HGW in the NCT gully along the lateral direction generally flowed away from the gully in the distance near the gully and then may flip the flow direction at the distance around the similar distance away from the gully. It appears that the distance of about 8 m away from the gully is a threshold. Within this distance, the magnitude of HWG flow for the rain periods was always larger around the CT gully than the NCT one. Yet beyond this distance, HWG around the CT gully still flowed in the same direction during the rain periods, while it reversed the direction around the NCT gully. During the dry periods, this threshold distance merely existed with *ET* values in class 1 (Fig. 9). Nonetheless, HWG mostly flowed toward the CT gully and away from the NCT gully except for *ET* values in class 4. This threshold behavior is consistent with the distance-decay effect of WT drawdown (Allott et al., 2009; Holden et al., 2006; Luscombe et al., 2016). Nonetheless, our results manifested that this effect mainly occurred around the CT gully. Furthermore, HGW consistently flowed out of the CT gully during the dry periods explained the larger amount of stored water lost around the CT gully (Fig. 13).

5. Conclusions

Groundwater storage and flow in peatland are very sensitive to climate change (both short and long terms) and topographic disturbance. Their spatial and temporal responses to these two factors are extremely hard to capture by *in situ* measurements. Alternatively, this study took on this issue by combining modeling analysis with limited, but sufficient field sampling. We investigated temporal changes of groundwater storage in the Zoige peatland and dynamic patterns of groundwater flows under the coupled influence of climate change and gullies. It was achieved by using Visual MODFLOW to simulate dynamics of groundwater movement in a peat zone with the area of 3.89×10^4 m^2 that included two deep (CT) gullies and a few shallow (NCT) gullies, as well as three sub-zones that had no gullies (NG), one NCT gully (NCT), and a CT gully (CT). The subsequent construction of water budget and analyses of vertical and horizontal groundwater flow provided new insight into the complex impact of climate change and gullies on groundwater storage and flows.

The short-term climate change is characterized by the oscillation of the difference between *P* and *ET* ($W_{P\text{-}ET}$). It controlled the frequent shift of loss and gain of groundwater storage in peatland during the wet season of a year. Yet, the fact that changes of groundwater storage (ΔS) during inter-rain periods were not correlated with *ET* values suggested that this control effect is more complicated: values of ΔS during a given inter-rain period are not only determined by the *ET* value, but also the ΔS value in its immediately earlier rain period. We call this as a hysteresis effect in groundwater processes. This effect is further confirmed by the fact that during inter-rain periods, peats in NG sub-zone lost more groundwater than NCT and CT sub-zones. During the wet season, though the impact of (short-term) climate change outweighed that of gullies on ΔS values, deep gullies significantly caused higher horizontal groundwater (HGW) flows in the areas near the gully, which is consistent with the well-known water table dropdown effect. Water table (WT) levels were strongly correlated with vertical groundwater (VGW) flows. However, ΔS values should not be significantly affected by variations of WT levels because VGW is negligible compared with HGW flows, which further raises question of determining ΔS using the

product of peat specific yield and the change of WT levels.

The effect of long-term climate change on ΔS values was represented by the continuous decrease of ΔS during the prolonged dry period. This impact is enhanced by deep gullies that may produce sustainable HGW flows, though the magnitudes of these flows may be small. Clearly, our findings highlight the critical role of deep gullies in reducing peat groundwater storage under both short-term and long-term climate changes. Future peatland restoration in the Zoige basin of China should focus on restricting development of existing (deep) gullies and preventing creation of new artificial ditches.

Declaration of Competing Interest

None.

Acknowledgements

This study was supported by the National Natural Science Foundation of China (51709020, 91647204, 91547112, 51622901), Open Project of State Key Laboratory of Plateau Ecology and Agriculture, Qinghai University (2017-KF-01), Project of Qinghai Science & Technology Department, Qinghai Province, China (2016-ZJ-Y01), Open Research Fund Program of State Key Laboratory of Hydroscience and Engineering, Tsinghua University, China (sklhse-2019-A-03), and Overseas Expertise Introduction Project for Discipline Innovation, China (D18013). We thank the full support of Prof. Hu Xuyue for field investigation and monitoring during the summers of 2016-2018. We also thank Xiang Li, Kaiyu Li, Youyong Li, Jing Liu, Yezhou Wu, and Xu Yan for field assistance and Yuchi You for preparing some figures. We appreciate three anonymous reviewers for their constructive comments.

Appendix A. Supplementary data

Supplementary data to this article can be found online at https://doi.org/10.1016/j.jhydrol.2019.05.032.

References

Abtew, W., Obeysekera, J., Iricanin, N., 2011. Pan evaporation and potential evapotranspiration trends in South Florida. Hydrol. Proc. 25 (6), 958–969.
Allen, R.G., Pereira, L.S., Raes, D., Smith, M., 1998. Crop Evapotranspiration Guidelines for Computing. Crop Water Requirements.
Allott, T.E.H., Evans, M.G., Lindsay, J.B., Agnew, C.T., Freer, J.E., Jones, A., Parnell, M., 2009. Water tables in Peak District blanket peatlands, Moors for the Future Report No. 17.' funded by the Environment Agency and National Trust. Hydrological benefits of moorland restoration.
Bai, J., Hua, O., Cui, B., Wang, Q., Chen, H., 2008. Changes in landscape pattern of alpine wetlands on the Zoige Plateau in the past four decades. Acta Ecol. Sin. 28 (5), 2245–2252.
Brixel, B., 2010. Quantification of the regional groundwater flux to a northern peatland complex, Schefferville, Québec, Canada: results from a water budget and numerical simulations. McGill University, Montréal, Québec, Canada.
Bujakowski, F., Falkowski, T., Wierzbicki, G., Zukowska, K., 2014. Using hydrodynamic modelling to assess the impact of the development on hydrogeological conditions in a polygenic river valley marginal zone. Ann. Warsaw University of Life Sci. – SGGW, Land Reclam. 46 (1), 43–55.
Burt, J.E., Barber, G.M., 2009. Elementary STatistics for Geographers, 3rd edition. The Guilford Press, New York.
Chason, D.B., Siegel, D.I., 1986. Hydraulic conductivity and related physical properties of peat, Lost River Peatlands, Northern Minnesota. Soil Sci. 142 (2), 91–99.
Cruz-Fuentes, T., Cabrera, M.D., Heredia, J., Custodio, E., 2014. Groundwater salinity and hydrochemical processes in the volcano-sedimentary aquifer of La Aldea, Gran Canaria, Canary Islands, Spain. Sci. Total Environ. 484, 154–166.
Cunliffe, A.M., Baird, A.J., Holden, J., 2013. Hydrological hotspots in blanket peatlands: Spatial variation in peat permeability around a natural soil pipe. Water Resour. Res. 49, 5342–5354.
Dahl, M., Nilsson, B., Langhoff, J.H., Refsgaard, J.C., 2007. Review of classification systems and new multi-scale typology of groundwater–surface water interaction. J. Hydrol. 344 (1–2), 1–16.
Evans, M., Warburton, J., 2007. Geomorphology of Upland Peat: Pattern, Process. Blackwell Publishing, Oxford, UK, Form, pp. 262.
Fisher, A.S., Podniesinski, G.S., Leopold, D.J., 1996. Effects of drainage ditches on vegetation patterns in abandoned agricultural peatlands in central New York. Wetlands 16 (4), 397–409.
Fraser, C.J.D., Roulet, N.T., Lafleur, M., 2001a. Groundwater flow patterns in a large peatland. J. Hydrol. 246 (1–4), 142–154.
Fraser, C.J.D., Roulet, N.T., Moore, T.R., 2001b. Hydrology and dissolved organic carbon biogeochemistry in an ombrotrophic bog. Hydrol. Proc. 15 (16), 3151–3166.
Gatis, N., Luscombe, D.J., Grand-Clement, E., Hartley, I.P., Anderson, K., Smith, D., Brazier, R.E., 2016. The effect of drainage ditches on vegetation diversity and CO2 fluxes in a Molinia caerulea-dominated peatland. Ecohydrology 9 (3), 407–420.
Grapes, T.R., Bradley, C., Petts, G.E., 2006. Hydrodynamics of floodplain wetlands in a chalk catchment: the River Lambourn, UK. J. Hydrol. 320 (3–4), 324–341.
Harbaugh, A.W., Banta, E.R., Hill, M.C., McDonald, M.G., 2000. MODFLOW-2000, the U. S. geological survey modular ground-water model—user guide to modularization concepts and the ground-water flow process, U.S. Geological Survey, Open-File Report 00-92, Reston, Virginia.
Hare, D.K., Boutt, D.F., Clement, W.P., Hatch, C.E., Davenport, G., Hackman, A., 2017. Hydrogeological controls on spatial patterns of groundwater discharge in peatlands. Hydrol. Earth Syst. Sci. 21 (12), 6031–6048.
Heathwaite, A.L., Göttlich, K. (Eds.), 1993. Mires: process, exploitation and conservation. John Wiley, Chichester.
Heathwaite, A.L., Johnes, P.J., 1996. Contribution of nitrogen species and phosphorus fractions to stream water quality in agricultural catchments. Hydrol. Proc. 10 (7), 971–983.
Holden, J., Burt, T.P., 2003. Hydraulic conductivity in upland blanket peat: measurement and variability. Hydrol. Proc. 17 (6), 1227–1237.
Holden, J., Chapman, P.J., Labadz, J.C., 2004. Artificial drainage of peatlands: hydrological and hydrochemical process and wetland restoration. Prog. Chem. Org. Nat. Prod. Phys. Geogr. 28, 95–123.
Holden, J., Chapman, P.J., Lane, S.N., Brookes, C., 2006. Impacts of artificial drainage of peatlands on runoff production and water quality. In: Martini, L.P., A. Martınez Cortizas, A., Chesworth, W. (Eds.), Peatlands: Evolution and Records of Environmental and Climate Changes. Elsevier, B.V., pp. 501–528.
Holden, J., Shotbolt, L., Bonn, A., Burt, T.P., Chapman, P.J., Dougill, A.J., Fraser, E.D.G., Hubacek, K., Irvine, B., Kirkby, M.J., Reed, M.S., Prell, C., Stagl, S., Stringer, L.C., Turner, A., Worrall, F., 2007. Environmental change in moorland landscapes. Earth-Sci. Rev. 82 (1–2), 75–100.
Holden, J., Wallage, Z.E., Lane, S.N., McDonald, A.T., 2011. Water table dynamics in undisturbed, drained and restored blanket peat. J. Hydrol. 402, 103–114.
Huo, L., Chen, Z., Zou, Y., Lu, X., Guo, J., Tang, X., 2013. Effect of Zoige alpine wetland degradation on the density and fractions of soil organic carbon. Ecol. Eng. 51, 287–295.
Jacobs, J.M., Mergelsberg, Shannon L., Lopera, Anderes F., Myers, David A., 2002. Evapotranspiration from a wet prairie wetland under drought conditions: Paynes prairie preserve, Florida, USA. Wetlands 22 (2), 374–385.
Joosten, H., Haberl, A., Schumann, M., 2008. Degradation and restoration of peatlands on the Tibet Plateau. PEATLANDS Int. 1, 31–35.
Kellner, E., Halldin, S., 2002. Water budget and surface-layer water storage in a sphagnum bog in Central Sweden. Hydrol. Proc. 16 (1), 87–103.
Labadz, J., Allott, T., Evans, M., Butcher, D., Billett, M., Stainer, S., Yallop, A., Jones, P., Innerdale, M., Harmon, N., Maher, K., Bradbury, R., Mount, D., O"Brien, H., Hart, R., 2010. Peatland Hydrology, Draft Scientific Review, commissioned by the IUCN UK Peatland Programme"s Commission of Inquiry on Peatlands.
Lautz, L.K., Siegel, D.I., 2006. Modeling surface and ground water mixing in the hyporheic zone using MODFLOW and MT3D. Adv. Water Resour. 29 (11), 1618–1633.
Li, J., Wang, W., Hu, G., Wei, Z., 2010. Changes in ecosystem service values in Zoige Plateau, China. Agric., Ecosyst. Environ. 139 (4), 766–770.
Li, Z., Gao, P., 2019. Impact of natural gullies on groundwater hydrology in the Zoige peatland, China. J. Hydrol.: Reg. Stud. 21, 25–39.
Li, Z., Gao, P., You, Y., 2018. Characterizing hydrological connectivity of artificial ditches in Zoige peatlands of Qinghai-Tibet Plateau. Water 10 (10), 1364.
Li, Z., Liu, X., Ma, T., De, K., Zhou, Q., Yao, B., Niu, T., 2013. Retrieval of the surface evapotranspiration patterns in the alpine grassland–wetland ecosystem applying SEBAL model in the source region of the Yellow River, China. Ecol. Modell. 270, 64–75.
Li, Z., Wang, Z., Brierley, G., Nicoll, T., Pan, B., Li, Y., 2015. Shrinkage of the Ruoergai Swamp and changes to landscape connectivity, Qinghai-Tibet Plateau. Catena 126, 155–163.
Lott, R.B., Hunt, R.J., 2001. Estimating evapotranspiration in natural and constructed wetlands. Wetlands 21 (4), 614–628.
Luscombe, D.J., Anderson, K., Grand-Clement, E., Gatis, N., Ashe, J., Benaud, P., Smith, D., Brazier, R.E., 2016. How does drainage alter the hydrology of shallow degraded peatlands across multiple spatial scales? J. Hydrol. 541, 1329–1339.
Mao, L.M., Bergman, M.J., Tai, C.C., 2002. Evapotranspiration measurement and estimation of three wetland environments in the Upper St. Johns River Basin, Florida. J. Am. Water Resour. Assoc. 38 (5), 1271–1285.
Millar, D.J., Cooper, D.J., Ronayne, M.J., 2018. Groundwater dynamics in mountain peatlands with contrasting climate, vegetation, and hydrogeological setting. J. Hydrol. 561, 908–917.
Molina, J.L., Pulido-Velazquez, D., Garcia-Arostegui, J.L., Pulido-Velazquez, M., 2013. Dynamic Bayesian Networks as a Decision Support tool for assessing Climate Change impacts on highly stressed groundwater systems. J. Hydrol. 479, 113–129.
Price, J.S., 1992. Blanket bog in Newfoundland. Part 2. Hydrological processes. J. Hydrol. 135, 103–119.
Price, J.S., 1996. Hydrology and microclimate of a partly restored cutover bog. Quebec. Hydrol. Proc. 10 (10), 1263–1272.
Price, J.S., Schlotzhauer, S.M., 1999. Importance of shrinkage and compression in determining water storage changes in peat: the case of a mined peatland. Hydrol. Proc.

13 (16), 2591–2601.
Price, J.S., Whitehead, G.S., 2001. Deveolping hydrological thresholds for Sphagnum recolonization on an abandoned cutover bog. Wetlands 21 (1), 32–40.
Putra, E.I., Cochrane, M.A., Vetrita, Y., Graham, L., Saharjo, B.H., 2018. Determining critical groundwater level to prevent degraded peatland from severe peat fire. In: Syartinilia (Ed.), 4th International Symposium on Lapan-Ipb Satellite for Food Security and Environmental Monitoring. IOP Conference Series-Earth and Environmental Science.
Ramchunder, S.J., Brown, L.E., Holden, J., 2009. Environmental effects of drainage, drain-blocking and prescribed vegetation burning in UK upland peatlands. Prog. Chem. Org. Nat. Prod. Phys. Geogr. 33 (1), 49–79.
Reeve, A.S., Gracz, M., 2008. Simulating the hydrogeologic setting of peatlands in the kenai peninsula lowlands. ALASKA. Wetlands 28 (1), 92–106.
Reeve, A.S., Siegel, D.I., Glaser, P.H., 2000. Simulating vertical flow in large peatlands. J. Hydrol. 227 (1–4), 207–217.
Ritzema, H., Jansen, H.C., 2008. Assessing the water balance of tropical Peatlands by using the inverse groundwater modelling approach. In: Farrell, C., Feehan, J. (Eds.), 13th International Peat Congress After Wise Use – The Future of Peatlands. Tullamore, Ireland, pp. 250–253.
Ronkanen, A.K., Klove, B., 2005. Hydraulic soil properties of peatlands treating municipal wastewater and peat harvesting runoff. Suo 56 (2), 43–56.
Ronkanen, A.K., Kløve, B., 2008. Hydraulics and flow modelling of water treatment wetlands constructed on peatlands in Northern Finland. Water Res. 42 (14), 3826–3836.
Rossi, P.M., Ala-aho, P., Doherty, J., Kløve, B., 2014. Impact of peatland drainage and restoration on esker groundwater resources: modeling future scenarios for management. Hydrogeol. J. 22 (5), 1131–1145.
Rossi, P.M., Ala-aho, P., Ronkanen, A.K., Klove, B., 2012. Groundwater-surface water interaction between an esker aquifer and a drained fen. J. Hydrol. 432, 52–60.
Shi, X., Thornton, P.E., Ricciuto, D.M., Hanson, P.J., Mao, J., Sebestyen, S.D., Griffiths, N.A., Bisht, G., 2015. Representing northern peatland microtopography and hydrology within the Community Land Model. Biogeosciences 12 (21), 6463–6477.
Sikstrom, U., Hokka, H., 2016. Interactions between soil water conditions and forest stands in boreal forests with implications for ditch network maintenance. Silva Fennica 50 (1), 1416.
Sumner, D.M., 2007. Effects of capillarity and microtopography on wetland specific yield. Wetlands 27 (3), 693–701.
Van Seters, T.E., Price, J.S., 2001. The impact of peat harvesting and natural regeneration on the water balance of an abandoned cutover bog, Quebec. Hydrol. Proc. 15 (2), 233–248.
Wang, M., Chen, H., Wu, N., Peng, C., Zhu, Q., Zhu, D., Yang, G., Wu, J., He, Y., Gao, Y., Tian, J., Zhao, X., 2014. Carbon dynamics of peatlands in China during the Holocene. Quat. Sci. Rev. 99, 34–41.
Wang, M., Yang, G., Gao, Y., Chen, H., Wu, N., Peng, C., Zhu, Q., Zhu, D., Wu, J., He, Y., Tian, J., Zhao, X., Zhang, Y., 2015. Higher recent peat C accumulation than that during the Holocene on the Zoige Plateau. Quat. Sci. Rev. 114, 116–125.
Whittington, P.N., Price, J.S., 2006. The effects of water table draw-down (as a surrogate for climate change) on the hydrology of a fen peatland, Canada. Hydrol. Proc. 20 (17), 3589–3600.
Wilson, L., Wilson, J., Holden, J., Johnstone, I., Armstrong, A., Morris, M., 2011. Ditch blocking, water chemistry and organic carbon flux: Evidence that blanket bog restoration reduces erosion and fluvial carbon loss. Sci. Total Environ. 409 (11), 2010–2018.
Wossenu, A., 1996. Evapotranspiration measurements and modeling for three wetland systems in South Florida. Water Resour. Bull. 32 (3), 465–473.
Xue, S., Liu, Y., Liu, S.L., Li, W.P., Wu, Y.L., Pei, Y.B., 2018. Numerical simulation for groundwater distribution after mining in Zhuanlongwan mining area based on visual MODFLOW. Environ. Earth Sci. 77 (11), 400.
Yang, G., Peng, C., Chen, H., Dong, F., Wu, N., Yang, Y., Zhang, Y., Zhu, D., He, Y., Shi, S., Zeng, X., Tingting, X., Meng, Q., Zhu, Q., 2017. Qinghai-Tibetan Plateau peatland sustainable utilization under anthropogenic disturbances and climate change. Ecosyst. Health Sustainability 3 (3), e01263.
Zheng, C., Bennett, G.D., 2002. Applied Contaminant Transport Modeling. Wiley-Interscience, New York.
Zhang, W., Lu, Q., Song, K., Qin, G., Wang, Y., Wang, X., Li, H., Li, J., Liu, G., Li, H., 2014. Remotely sensing the ecological influences of ditches in Zoige Peatland, eastern Tibetan Plateau. Int. J. Remote Sens. 35 (13), 5186–5197.
Zhang, X., Schumann, M., Gao, Y., Foggin, J., Wang, S., Joosten, H., 2016. Restoration of high-altitude peatlands on the Ruoergai Plateau (Northeastern Tibetan Plateau, China). In: Bonn, A., Allott, T., Evans, M., Joosten, H., Stoneman, R. (Eds.), Peatland Restoration and Ecosystem Services: Science, Policy and Practice. Cambridge University Press, Cambridge, pp. 234-252. doi:10.1017/CBO9781139177788.014.
Zhao, Y., Tang, Y., Yu, Z., Li, H., Yang, B., Zhao, W., Li, F., Li, Q., 2014. Holocene peatland initiation, lateral expansion, and carbon dynamics in the Zoige Basin of the eastern Tibetan Plateau. Holocene 24 (9), 1137–1145.